

Disk galaxy rotation curves and dark matter distribution*

Dilip G. Banhatti

After explaining the motivation for this article, I briefly recapitulate the methods used to determine, somewhat coarsely, the rotation curves of our Milky Way Galaxy and other spiral galaxies, especially in their outer parts, and the results of applying these methods. Recent observations and models of the very inner central parts of galaxian rotation curves are only briefly described. I then present the essential Newtonian theory of (disk) galaxy rotation curves. The next two sections present two numerical simulation schemes and brief results. Application of modified Newtonian dynamics to the outer parts of disk galaxies is then described. Finally, attempts to apply Einsteinian general relativity to the dynamics are summarized. The article ends with a summary and prospects for further work in this area.

Keywords: Dark matter, Milky Way, rotation curves, spiral galaxies.

Motivation

Extensive radio observations determined the detailed rotation curve of our Milky Way Galaxy as well as other (spiral) disk galaxies to be flat, much beyond their extent as seen in the optical band. Assuming a balance between the gravitational and centrifugal forces within Newtonian mechanics, the orbital speed V is expected to fall with the galactocentric distance r as $V^2 = GM/r$, beyond the physical extent of the galaxy of mass M , G being the gravitational constant. The run of V against r , for distances less than the physical extent, then leads to the distribution $M(r)$ of mass within radius r . The observation $V \approx \text{constant}$ for large enough r , up to the largest r , up to 100 kpc, thus shows that there is substantial amount of matter beyond even this largest distance. A spherically symmetric matter density $\rho(r) \propto 1/r^2$, characteristic of an isothermal ideal gas sphere, naturally leads to $V = \text{constant}$. Since this matter does not emit radiation, it is called dark matter. In general, the existence of dark matter is, by astrophysical definition, inferred solely from its gravitational effects. (Astro)particle physicists¹ hope to change this by directly detecting dark-matter particles. Considering the evidence for different types of dark matter on scales from our solar system out to the observable universe², the detailed structure on the sky of cosmic microwave background radia-

tion³, simulations for large-scale structure formation⁴, and big-bang nucleosynthesis calculations⁵, such gravitationally and otherwise normally interacting dark matter may be made of very light normal particles, like (massive) neutrinos, which are relativistic (and hence called hot dark matter) or much heavier (about a GeV/c^2 or more) exotic nonrelativistic particles (hence called cold dark matter)⁶. By ‘exotic’ here I mean not any of the particle zoo of the standard model of particle physics⁶. For an exposition regarding our current picture of the composition of the universe and other details, see e.g. Grupen¹ and references therein. Here, we confine our attention to the scale of individual galaxies.

One often assumes an isothermal dark matter halo, although $\rho(r) \propto 1/r^2$ is only one of the many density profiles leading to $V = \text{constant}$, the others being disk-like. For disk-like mass distributions, in contrast to spherically symmetric ones, the circular speed at a given r is deter-

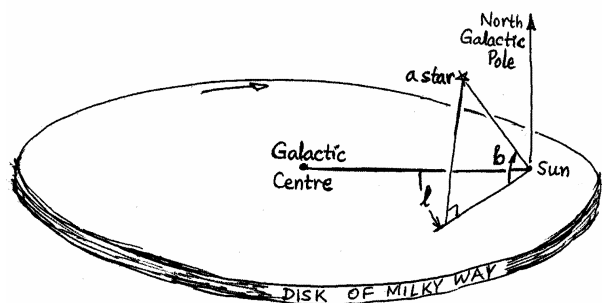


Figure 1. A schematic picture of Sun’s location in the Milky Way Galaxy, illustrating galactic coordinates b (latitude) and l (longitude). Rotation is indicated by an arrow.

*Based on a pedagogic/didactic seminar given at the Graduate College ‘High Energy and Particle Astrophysics’ at Karlsruhe, Germany on 20 January 2006.

Dilip G. Banhatti is in the School of Physics, Madurai Kamaraj University, Madurai 625 021, India.

Present address: Solid State Theory group at University of Münster, Germany. e-mail: dilip.g.banhatti@gmail.com

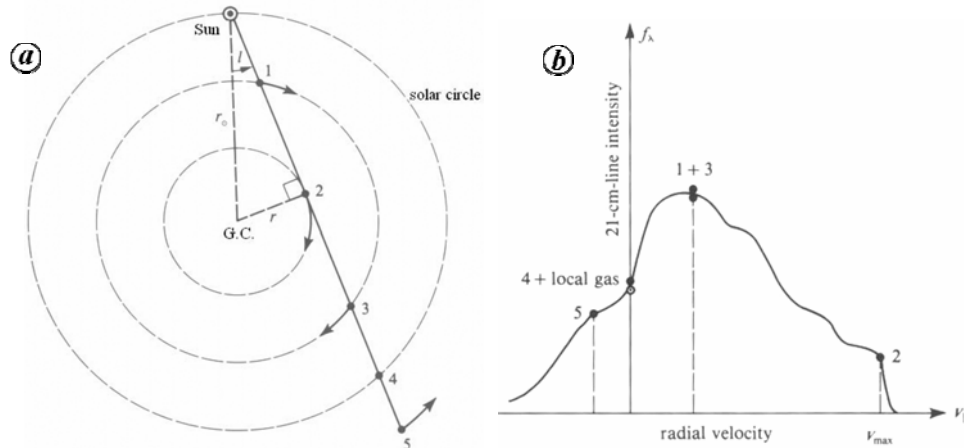


Figure 2. *a*, Different types of clouds in a given direction. *b*, Neutral hydrogen line profile showing typical regions as numbered in (*a*).

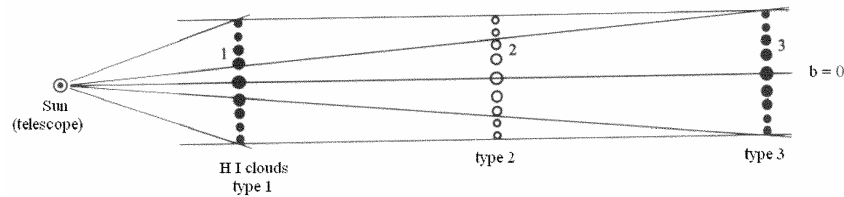


Figure 3. Resolving distance ambiguity by comparing widths in Galactic latitude.

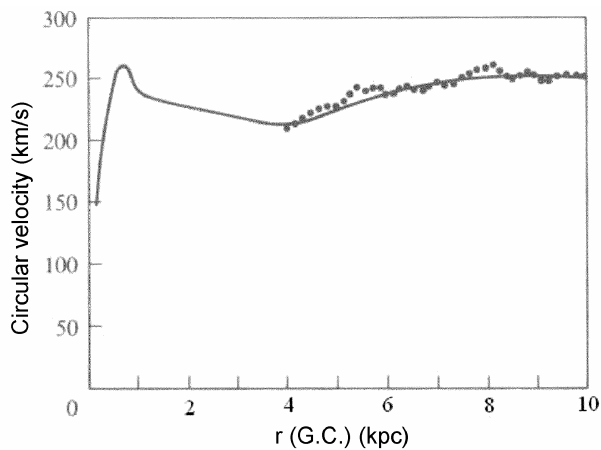


Figure 4. Milky Way rotation curve in the outer parts.

mined by matter distributed from 0 to r and also beyond r , as can be easily seen by applying Gauss' integral theorem (or law) to appropriately shaped closed volumes. Some textbooks make the error of integrating only up to r , leading to wrong results, as pointed out by Méra *et al.*⁷

Recently, de Boer *et al.*⁸ reanalysed the public domain data from the 0.1 to 10 GeV all-sky γ -ray survey, which

was done by the satellite-borne telescope EGRET. They found that excess diffuse γ rays of the same spectrum are observed in all the sky directions, and that the spectral shape can be interpreted as annihilation of (dark matter) particles (and antiparticles) into intermediaries like π^0 mesons and then to γ -ray photons, implying a mass of 60–70 MeV/ c^2 for the annihilating (dark matter weakly interacting massive) particle (or antiparticle). From the intensity variation of the diffuse γ -ray excess with respect to Galactic longitude and latitude (Figure 1), and assuming a spherically symmetric component in the mass distribution, they derived an almost spherical isothermal profile plus substructure in the Galactic Plane in the form of two toroidal rings at 4.2 and 14 kpc from the Galactic Centre. (The absolute normalization of the dark-matter profile is tied to the local rotation speed 220 km/s at 8.3 kpc, the Sun's distance from the Galactic Centre. This may need renormalization for consistency with better and more recent determinations, e.g. like those of Xu *et al.*⁹ and Hachisuka *et al.*¹⁰.) The two rings produce, within Newtonian dynamics, the observed bumps in the detailed shape of the Galactic rotation curve. These rings are actually broken segments disposed around the Galactic Centre in ring-like structures, as also seen for OB stellar associations via their distribution and kinematics¹¹. In general, nonaxisymmetric structures like spiral arms and bars should also

be taken into account¹². Dekel¹³ cautions to choose carefully test particles to measure rotation curves in general, giving an example where low stellar speeds turn out to be a red herring, detailed disks' merger model for the elliptical galaxies in question showing orbits consistent with dark matter halo and low stellar speeds. Aharonian *et al.*¹⁴ describe the discovery of TeV γ -rays from the Galactic Centre Ridge. Ando¹⁵ treats cosmic γ -rays as being from dark matter annihilation. In this article, I restrict myself to outer parts of galaxies, i.e. to sufficiently large r , where the rotation curve has stabilized to a flat shape on average.

Measurements in the Milky Way Galaxy^{16,17}

In the kinematic method of determining distances in the Galactic Plane in a given direction (Figure 2), the radial speeds of neutral hydrogen (i.e. H I \equiv H⁰) clouds are measured by the Doppler shifts of the $\lambda 21$ cm line corresponding to the electronic spin-flip transition of the H atom. The highest radial speed in the line profile in Galactic longitude direction ℓ gives the circular rotation speed V at distance $r = r_{\text{Sun}} \sin \ell$ from the Galactic Centre. The distance ambiguity for clouds of types 1 and 3 is removed (or resolved) by measuring their extent in Galactic latitude (Figure 3). Another way is to measure hydrogen absorption at radio frequencies, since distant sources show wider velocity range¹⁸. Such measurements give the Milky Way rotation curve in its outer parts, up to about the Solar Circle, as shown in Figure 4. Relative to the Sun (i.e. a frame of reference rotating with angular speed $\Omega(r_{\text{Sun}})$), the circular speed of a gas cloud at radius r is $r[\Omega(r) - \Omega(r_{\text{Sun}})]$ (Figure 5). The line of sight speed V_{\parallel} at a given Galactic latitude ℓ is $V_{\parallel} = r[\Omega(r) - \Omega(r_{\text{Sun}})]\sin(\theta + \ell) = r_{\text{Sun}}[\Omega(r) - \Omega(r_{\text{Sun}})]\sin \ell$.

Thus $V(r) = r\Omega(r) = V_{\text{max}} + r_{\text{Sun}}\Omega(r_{\text{Sun}})\sin \ell$, where V_{max} is the maximum value of V_{\parallel} from the line profile. Beyond

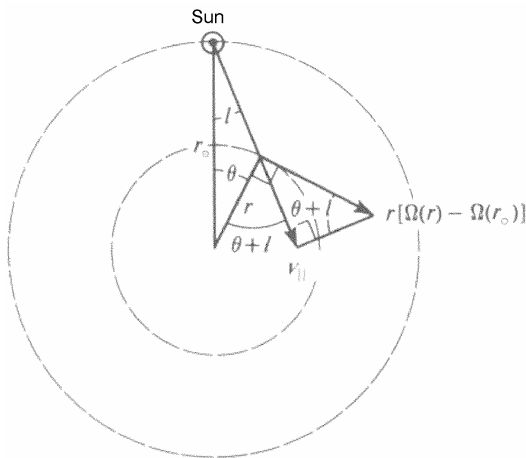


Figure 5. Geometry to calculate kinematic distances in the Galactic Plane.

Solar Circle $r = r_{\text{Sun}}$, giant H II \equiv H⁺ complexes are used in place of H I (\equiv H⁰) regions. The tracers for these complexes are the CO line (at $\lambda \approx 1-3$ mm) and H109 α (at $\lambda 6$ cm), among others. Figure 6 shows the Milky Way rotation curve beyond the Solar Circle, with the 'expected' curves for uniform (i.e. rigid body) rotation in the inner part and Keplerian behaviour in the outer part. Coarse observations, when interpolated across the nucleus, correspond roughly to uniform or rigid-body rotation in the inner part, although the recently discovered finer-scale structure there has other implications¹⁹. Briefly, molecular and maser line spectroscopy of massive inner nuclear disks has shown the presence of order of magnitude larger Keplerian speeds than the outer 'flat' value, indicating a possible supermassive nuclear black hole. Bar kinematics has been inferred from detailed observations. Even counter-rotating nuclear disks, possibly resulting from mergers, are present. Perhaps the nuclear black hole has 'sucked in' these peculiarities of structure and kinematics to leave more orderly (flat) rotational kinematics in the outer parts of (spiral) galaxies. The reader can refer to the literature for recent observational details²⁰. In the outer part, the rotation speed is clearly super-Keplerian, on average flat, with some modulations, in this plot (Figure 6) from Shu¹⁶. Binney and Tremaine¹⁷ summarize the detailed disk surface mass density model of Caldwell and Ostriker²¹, which is essentially a fit with 13 observationally determined parameters:

$$\sigma(R) = \sigma_0[\exp(-R/R_1) - \exp(-R/R_2)].$$

The central model density is zero, which cannot accommodate a central mass concentration, for which there is ample independent evidence¹⁹. However, the model has toroidal rings at R_1 and R_2 for which there is separate observational evidence^{8,11} as mentioned earlier. So a super-

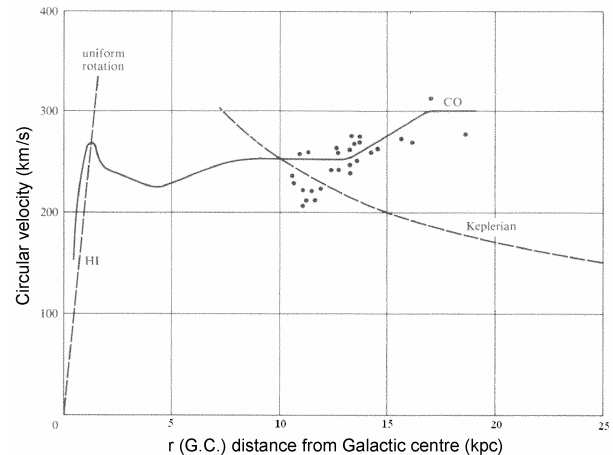


Figure 6. Milky Way rotation curve beyond the Solar Circle. Uniform rotation means rigid-body rotation $v = \omega \cdot r$, with uniform angular speed ω , independent of r .

position of such a model with another component having centrally concentrated mass should fit the observed rotation curve for inner as well as outer parts of the Milky Way Galaxy. For other detailed models of (especially the outer parts of) the Milky Way rotation curve, see Cowsik *et al.*²² and Dehnen and Binney²³.

Rotation curves of other galaxies

Assuming Newtonian gravitation to predominantly determine the dynamics, the mass M may be estimated from orbital speed V in ellipticals as well as spirals. The mass M interior to r is roughly $M(r) = rV^2/G$, with r the deprojected distance and V the (spread in) random speeds for ellipticals, while in spirals it refers to the circular speed about the galaxian centre. For a disk galaxy it is more meaningful to take $M(R)$ as the mass within a cylinder of radius R , while for a spheroidal galaxy $M(r)$ is more conveniently the mass within a sphere of radius r . Observationally, measurements are possible only along the total line-of-sight through a galaxy (Figure 7). Thus the cylindrical radius is more pertinent for observations. However, the practical difference between the two is not large for actual galaxies, as is seen from the following example. Take $\rho(r) = C/r^2$. Then the surface mass density is

$$\begin{aligned} \sigma(R) &= \int_{\text{all } z} dz \rho(r), \quad \text{where } r^2 = R^2 + z^2 \text{ (Figure 7)} \\ &= \pi C/R. \end{aligned}$$

Hence the masses within a sphere of radius r and a cylinder of radius R are

$$\begin{aligned} M_{\text{sph}}(r) &= \int_0^r dr 4\pi r^2 \rho(r) = 4\pi Cr \quad \text{and} \\ M_{\text{cyl}}(R) &= \int_0^R dR 2\pi R \sigma(R) = 2\pi^2 CR. \end{aligned}$$

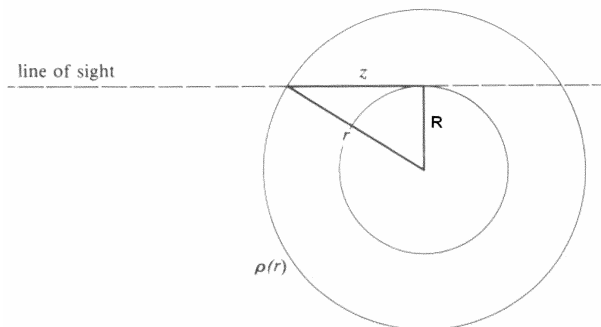


Figure 7. Line-of-sight through a galaxy showing the relation between spherical radius r and cylindrical radius R .

For $r = R$, $M_{\text{sph}}/M_{\text{cyl}} = 2/\pi \sim 1$. This is only relevant for observations. Dynamically, even for disk geometry, the relevant quantity is $M_{\text{sph}}(r)$, as one can see by applying Gauss’ law to appropriately shaped closed volumes, as emphasized earlier.

In general, (radio) line observations give data on the intensity (and possibly polarization) of the targetted emitting matter in very many velocity (as implied by shifted frequency) channels in each pixel \equiv restoring beam. These data can be viewed and plotted in many different ways. The two most popular presentations give (1) a (polarized or total) intensity contour map with colour-coded iso-velocity contours superposed (Figure 8; called spider diagram), and (2) a cut through such a map showing a plot of velocity vs distance along the cut (Figure 9; called position–velocity or PV plot).

The velocity is always corrected for projection using an estimate of the inclination angle of the disk to the line-of-sight. There are other ways of getting the rotation curve, defined as such a position–velocity plot¹⁹. A neutral hydrogen (i.e. H^0) study²⁴ of NGC 6744 out to 40 kpc is shown in Figure 10. UGC2885, NGC 5533 and NGC6674 rotation curves are measured²⁵ to ~ 70 kpc.

In the radio band, rotation curves can be measured out to about 2–3 Holmberg radii²⁷, while in the optical band it is possible to measure only to about 0.5 times the Holmberg radius. The Holmberg radius corresponds to the isophote at a specific well-defined low surface brightness, about 1–2% above the background sky brightness¹⁷. Other scales used to gauge the extent of disk galaxies are exponential disk scale length r_d from I-band photometry and the radius R_{opt} encompassing 83% of the total integrated light, fruitfully used by Catinella *et al.*²⁸, who constructed template rotation curves by combining data on about 2200 disk galaxies, fitting for the amplitude V_0 , exponential scale r_{pe} of the inner region and slope α of the outer part:

$$V_{\text{pe}}(r) = V_0 [1 - \exp(-r/r_{\text{pe}})] (1 + \alpha r/r_{\text{pe}}),$$

pe, representing ‘polyex’, the name of the model, and r and r_{pe} expressed in units of r_d or R_{opt} . Detailed mapping

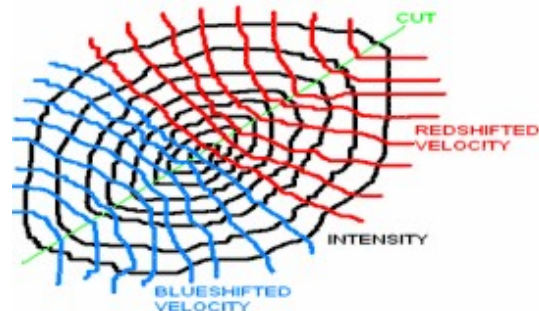


Figure 8. Schematic representation of iso-velocity contours superposed on intensity contour map (spider diagram).

of radial distribution of visible and dark matter in disk galaxies requires use of luminosity profiles and extended H^0 rotation curves in addition to optical rotation curves. Martín²⁷ has collated H^0 maps from the literature published between 1953 and 1995, into a uniform catalogue of about 1400 disk galaxies, and has analysed some of the data in an attempt to derive features and relations common to most galaxies. It is sufficient to use angular distances (arcminutes or arcseconds) for the radial distances r , r_{pe} , r_d and R_{opt} for such compilations. A translation to physical units (kpc) is needed only for going to mass models. From a study of a homogeneous sample of about 1100 optical and radio rotation curves and relative surface photometry, Persic *et al.*²⁹ found that a single property like total luminosity dictates the rotation velocity at any radius for any galaxy, revealing the existence of a universal rotation curve, which they derived, confirming their result from an earlier study based on 58 rotation curves. However, Bosma³⁰ cautions that derivation of any universal rotation curve may not be warranted. See also recent evidence for two halo components in a galaxy, one of them retrograde²⁰. I also mention Narayan and Jog³¹ in this connection, who show how the convenience of presenting intensity vs radius as a log-linear plot led to a spurious observational cut-off to the luminous disk, promptly taken up by theorists to construct elaborate

models! Different ways of presenting astrophysical data are essential for many purposes, as, for example, done by Kundt³², who presented rotation curves in a novel way.

(Newtonian) theory of (disk) galaxy rotation curves

Binney and Tremaine¹⁷ have given a detailed treatment of observations, models and theory of galaxian dynamics within Newtonian gravitational and dynamical framework. Saslaw³³ has treated gravitational systems in general from a much broader perspective, and, in the process, given a concise summary of the essential Newtonian methodology. The reader can refer to these (and other possibly more recent) studies for details. Here only a few glimpses are given, hopefully enough to whet the appetite for more.

Relation between $\Phi(r)$ and $\rho(r)$ [or $V^2(r)$ and $M(r)$]

The gravitational potential energy per unit mass is called Newtonian gravitational potentials Φ . This is only a convenient mathematical quantity and has no physical existence in Newtonian theory, which is a simultaneous far-action theory rather than (special) relativistically propagating field theory like (classical) electromagnetism. (See Graneau and Graneau³⁴ for an elaboration of this point. See also Banhatti and Banhatti³⁵.)

For a test particle in a circular orbit at radius r in a spherically symmetric mass distribution $\rho(r)$, the circular speed $V(r)$ is found from

$$V^2(r) = r d\Phi/dr = rF = GM(r)/r = (4\pi G/r) \int_0^r dr' r'^2 \rho(r'),$$

where F is the (radial) force/unit mass, and $M(r)$ the mass within a sphere of radius r . The escape speed $V_e = (2|\Phi(r)|)^{1/2}$, since the kinetic and potential energies are just balanced at this speed.

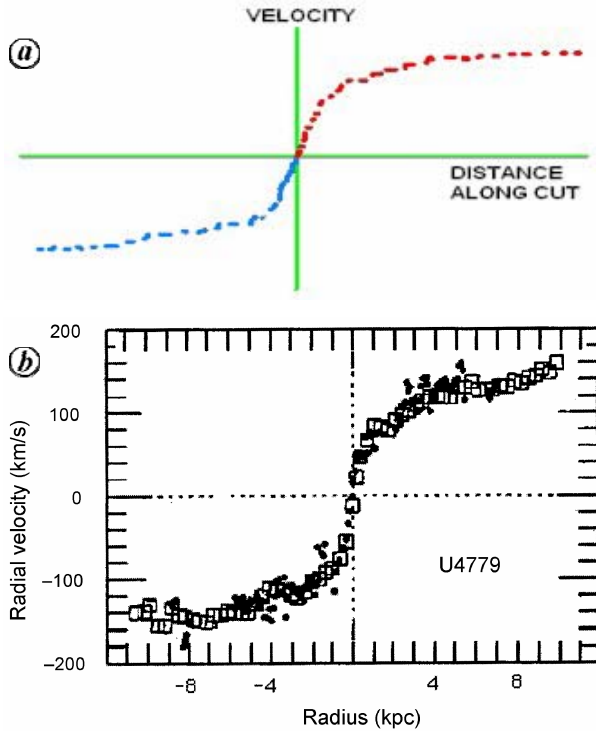


Figure 9. *a*, Schematic galaxy rotation curve (PV plot), such as may be derived from a spider diagram like in Figure 8 by integrating or taking a one-dimensional section. *b*, An observed galaxy rotation curve²⁶ for UGC4779 = NGC2742.

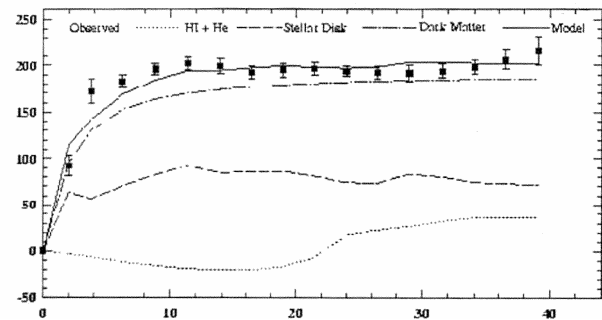


Figure 10. Rotation curve of NGC6744 to large galactocentric distance. (Velocity in km/s vs deprojected distance in kpc; from Ryder *et al.*²⁴).

Potential ↔ density pairs (and other quantities)

Spherically symmetric: For illustration, some simple potentials are listed.

Point mass M : $\Phi(r) = -GM/r$, $V(r) = (GM/r)^{1/2}$ and $V_e(r) = (2GM/r)^{1/2}$.

Homogeneous sphere: $M(r) = (4/3)\pi r^3 \rho$, with ρ uniform (i.e. independent of r) and $V(r) = (4\pi G\rho/3)^{1/2}r$, rising linearly with radius. The orbital period is $T = 2\pi r/V = (3\pi/G\rho)^{1/2}$, independent of radius r . A test mass released at r oscillates harmonically around $r = 0$, where it reaches after $t_{\text{dyn}} = T/4 = (3\pi/16G\rho)^{1/2}$, the dynamical time of a system of mean density ρ . For radial size a ,

$$\Phi(r) = \begin{cases} -2\pi G\rho(a^2 - r^2/3), & r \leq a \\ -4\pi G\rho a^3/3r, & r \geq a \end{cases}.$$

Other systems of interest are¹⁷ isochrone potential, modified Hubble profile and power-law density.

Flattened systems: Plummer–Kuzmin, Toomre’s n and logarithmic. For details, see Binney and Tremaine¹⁷.

Poisson’s equation for thin disks: For an axisymmetric system with density $\rho(R, z)$,

$$\partial^2\Phi/\partial z^2 = 4\pi G\rho(R, z) + (1/R)(\partial/\partial R)(RF_R); F_R \equiv -\partial\Phi/\partial R$$

being the radial force.

Near $z = 0$, the first term on the RHS \gg the second term, so that $\partial^2\Phi/\partial z^2 = 4\pi G\rho(R, z)$.

So Poisson’s equation for a thin disk can be solved in two steps: (1) Using surface density (zero thickness), determine $\Phi(R, 0)$. (2) At each radius R , solve this simplified Poisson’s equation for the structure normal to the disk.

Disk potentials: By separating variables in cylindrical polar coordinates, surface density $\sigma(R)$ and potential $\Phi(R, z)$ are related by

$$\Phi(R, z) = -2\pi G \int_0^\infty dk \exp(-k|z|) J_0(kR) \times \int_0^\infty dR' R' \sigma(R') J_0(kR'),$$

where J_0 is a Bessel function. Writing

$$S(k) = -2\pi G \int_0^\infty dR R \sigma(R) J_0(kR),$$

the circular speed is given by

$$V^2(R) = R(\partial\Phi/\partial R)_{z=0} = -R \int_0^\infty dk k S(k) J_1(kR), \text{ using}$$

$$dJ_0(x)/dx = -J_1(x).$$

Examples applying these formulae: Rotation curve of Mestel’s³⁶ disk: $\sigma(R) = \sigma_0 R_0/R$.

Calculation gives uniform, i.e. R -independent, circular speed: $V^2 = 2\pi G\sigma_0 R_0$.

Since

$$M(R) = 2\pi \int_0^R dR' R' \sigma(R'),$$

this can also be written $V^2 = GM(R)/R$, as for a spherical system, which is true only for Mestel’s disk.

Exponential disk: $\sigma(R) = \sigma_0 \exp(-R/R_d)$.

Calculation gives $V^2(R) = 4\pi G\sigma_0 R_d y^2 [I_0(y)K_0(y) - I_1(y)K_1(y)]$, where $y \equiv R/2R_d$, and I_0, K_0, I_1, K_1 are Bessel functions.

Deducing $\sigma(R)$ given $V(R)$ is formally possible, but involves differentiating the noisy observed function $V^2(R)$, which numerically worsens the error and is unstable.

Fourier (numerical) method in cylindrical polar coordinates³⁷

With $u \propto \ln R$, a rectangular grid in the (u, φ) plane, where $-\infty < u < \infty$ and $0 \leq \varphi$ (the azimuthal angle) $\leq 2\pi$, generates, in the (R, φ) plane, cells that become smaller as $R \rightarrow 0$. This is well suited to (numerical simulations of) centrally concentrated disks. A particularly efficient implementation is Miller’s code³⁸ using ‘leapfrog’ numerical scheme, called Verlet method in molecular dynamics, extensively used at Turku (Finland) and later³⁹ for various aspects of disk galaxies, including spiral arms, tidal interactions, Seyfert activity, etc. The N -body code uses 60,000 particles in a smoothed potential. The particles are distributed on a 24×36 standard grid (part of which is shown in Figure 11), determined by $r = L \exp(\lambda u)$; $\lambda = 2\pi/36$ and u ranging from 0 to 23.5, so that r ranges from L to $60.4L$.

The initial disk has

$$\sigma(R) = \begin{cases} [V_0^2/\pi GR] \cos^{-1}(R/A) & \text{for } R \leq A \\ 0 & \text{for } R \geq A \end{cases};$$

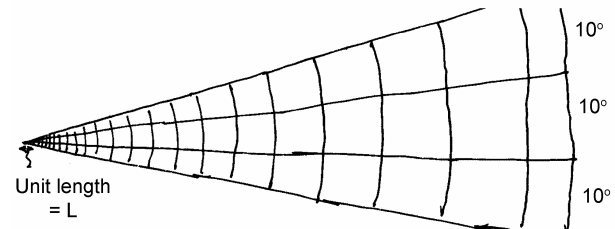


Figure 11. Two-dimensional polar coordinate grid used in Miller’s numerical code³⁸.

where $A \equiv$ disk radius. (See Grupen¹, eq. (13.7), p. 268, where one finds a concise summary of disk galaxy dynamics vis-à-vis motivation for dark matter.)

Thus the circular speed V_0 is, by integrating $\sigma(R)$ to get the total galaxy mass M , given by

$$V_0^2 = \pi GM/2A. \text{ The potential/unit mass is}$$

$$\Phi(R) = \begin{cases} V_0^2 \ln(R/2A) & \text{for } R \leq A \\ -(2V_0^2/\pi) \sum_{\ell=0}^{\infty} [1 \cdot 3 \cdot 5 \cdots (2\ell + 1) / \{2^\ell \ell! (2\ell + 1)^3\}] (A/R)^{(2\ell+1)} & \text{for } R > A \end{cases}$$

The action of a spherical halo of density $\propto 1/r^2$ is the same as if it was projected on the disk plane, as can be verified by calculation that the surface density of the projected halo has the same form as assumed. In fact, this is the motivation for using this form. The halo acts on the disk, but is not acted on, either by itself or by the disk. This is somewhat puzzling and may give spurious effects.

Disk halo break-up and a new calculation scheme⁷

Poisson's equation is numerically solved for an axially symmetric disk in cylindrical polar coordinates, using 250,000 points = particles distributed along 500 rings of radii $\propto i^2$, where i is the ring number from the centre outward, up to R_g , the radius of the finite disk. The force $\mathbf{F} \propto \int [\sigma(R)/R^3] \mathbf{R} d\mathbf{R}$ acting on a given particle is discretized to

$$\mathbf{F}_i = \sum_{j \neq i} G(m_i m_j / d_{ij}^3) \mathbf{d}_{ij}, \text{ where } \mathbf{d}_{ij} = \mathbf{x}_j - \mathbf{x}_i.$$

also

$$= m_i (v_i^2 / d_i) (\mathbf{x}_i / d_i) \text{ to give the rotation curve, } i = 0, 1, \dots, n.$$

$$d_{ij}^2 = d_i^2 + d_j^2 - 2d_i d_j \cos(\theta_{ij}),$$

so that with

$$F_{ij} = G(d_i - d_j \cos \theta_{ij}) / d_{ij}^3,$$

the set of equations reduces to $\sum_{j \neq i} m_j F_{ij} = v_i^2 / d_i$. This is a system of n linear equations, with $n + 1$ unknowns m_i (since we seek to invert $V^2 \rightarrow \sigma$). The additional equation needed is provided by the total mass M_g of the galaxy: $M_g = \sum_i m_i$. Writing $\mu_i = m_i / M_g \equiv \omega m_i$, the $n + 1$ equations for $n + 1$ unknowns μ_i , for each value of ω , are (for $i = 1, \dots, n$) ($i = 0$ gives $\mathbf{0} = \mathbf{0}$):

$$\sum_{j=0 (j \neq i)}^n m_j F_{ij} = \omega v_i^2 / d_i, \quad \sum_{j=0}^n \mu_j = 1,$$

with the constraint $\mu_i \geq 0$.

The constraint restricts ω between ω_{\min} and ω_{\max} , which are close to each other (within 10^{-2} or less). The physical significance of the existence of the free parameter ω is that the rotation curve is known only up to R_g , the radius of the finite disk. The range allowed for ω corresponds to all possible extensions of the rotation curve beyond R_g . Since the range of ω is narrow, the mass of the galaxy from the known rotation curve is naturally found.

The method has been tested successfully for exponential disk, point mass and Mestel's disk. Figure 12 shows the surface density $\sigma(R)$ for the Milky Way derived in this way from the rotation curve of Vallée⁴⁰. $R_g = 14$ kpc is used from Robin *et al.*⁴¹. Comparison with other results and taking into account MACHO gravitational lensing candidates toward LMC, a halo of the same radius as the disk is needed.

However, as Méra *et al.*⁴² (and references therein) show in detail using star counts, microlensing observations and kinematics, the model eventually to be found consistent with all constraints is not yet determined, although both maximal halo-type models with non-baryonic (i.e. exotic) dark matter and maximal disk-type models with all matter baryonic are possible.

Gentile *et al.*⁴³ use H^0 and $H\alpha$ data on five spirals to decompose the rotation curve into stellar, gaseous and dark matter contributions, pointing toward halos with constant density cores.

MoND and disk galaxy rotation curves⁴⁴

MoND was proposed in 1983 as a phenomenological model to fit gross features of rotation velocity data for spirals, especially Tully–Fisher relation $M(\text{mass}) \propto V^4$, V denoting the flat value of the outermost part of the rotation curve. The idea behind MoND was to seek a low field value a_0 ($\approx 10^{-8} \text{ cm/s}^2$, as it turns out), which modifies Newtonian gravitational acceleration (or field) from g_N to $(g_N a_0)^{1/2}$ for low gravitational fields. As it happens, $a_0 \approx cH_0/6$, with c the speed of light and H_0 the Hubble constant. Detailed variation of spiral rotation curves fits well with only one additional parameter giving the mass-to-light ratio across the whole spiral disk. Thus evidence for dark matter from spiral rotation curves can equally well be interpreted as evidence for MoND, which may at worst be taken to be a parametrization of rotation curve data, which a more fundamental model or theory should account for. The search is still on for such a physical basis (in the form of a field theory) for this acceleration (i.e. gravitational field)-based modification of Newtonian dynamics (and inertia). Recently⁴⁵, a unification of dark matter and dark energy into a dark fluid described by a tensor–

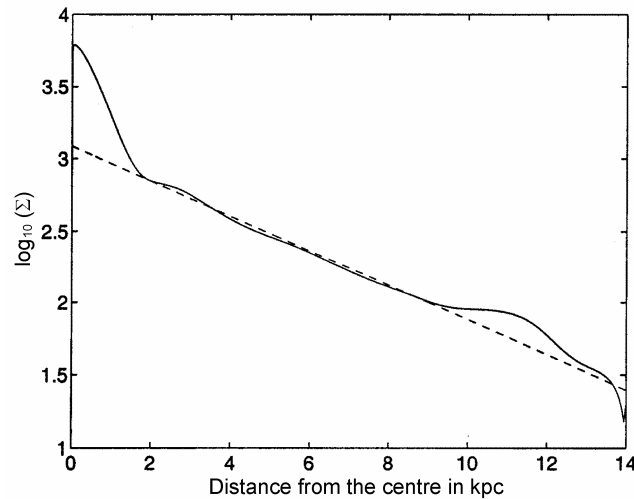


Figure 12. Surface mass density for Milky Way Galaxy compared with the model of Méra *et al.*⁷ (dotted). (The same figure is also available in Méra *et al.*⁴² as figure 2.)

vector–scalar (TeVeS) field theory has consonance with MoND. For details, see Sanders and McGaugh⁴² and Zhao⁴⁵.

General relativity vs Newtonian gravity and dynamics

Newtonian gravity and dynamics together form a simultaneous far-action theory. Newtonian gravitational potential (energy) is essentially a force field, giving the force/unit mass in space. This is true despite application of sophisticated mathematical techniques, as there is no (special) relativistic field propagation in Newtonian theory, which is not Lorentz-invariant, but Galilean, with absolute simultaneity, and space and time independent of each other. General relativity, on the other hand, is locally Lorentz-invariant, and is a genuine field theory with relativistic field propagation built into its structure.

Galaxy rotation curves

A galaxy is modelled as a stationary axially symmetric pressure-free fluid in general relativity. The rotation curve is derived by tracing paths of test particles, i.e. determining geodesics. The recent claim by Cooperstock and Tieu⁴⁶ that such a procedure leads to a good fit to observed galaxy rotation curves, without having to assume the existence of exotic dark matter, has been shown to be misguided by Vogt and Letelier⁴⁷, who infer that matter of negative energy density is implied in the disk. Korzyński⁴⁸ has shown that a singular disk is implied. Cross⁴⁹ found that correcting an internal inconsistency no longer leads to a flat rotation curve. Fuchs and Phelps⁵⁰ have pointed out the inadequacy of the model to reproduce

local mass density and vertical density profile of the Milky Way. However, the idea of treating the nonlinear galactodynamical problem using general relativity rather than Newtonian gravity, due to the inherent nonlinearity of self-gravity and (general relativistic) dragging of inertial frames in the rotating model spacetimes, is well worth pursuing further. An example is Vogt and Letelier⁵¹. Another is Balasin and Grumiller⁵², who point out that the Newtonian approximation breaks down globally, even though it is valid locally everywhere, confirming Fuchs and Phelps' failed attempt⁵⁰ to apply the model to the Milky Way Galaxy. Letelier⁵³ has summarized the position, also referring to an earlier relevant study by González and Letelier⁵⁴. Finally, it is worth mentioning Gödel's study of rotating spacetimes, examined from a broader perspective by Yourgrau⁵⁵. See also Banhatti⁵⁶.

Summary/conclusion

Galaxy rotation curves are flat to the greatest extent they can be measured. Precise observations have delineated the undulations in this overall flat structure, especially for the Milky Way Galaxy. The low-field theory MoND phenomenologically fits details of disk rotation curves surprisingly well, with the same mass-to-light ratio across the whole disk as the only galaxian parameter, along with a constant low-field value, the constant acceleration of about 10^{-8} cm/s², intrinsic to MoND.

There is a direct relation between rotation curves and mass models for galaxies. Dark matter is probably needed to fit the observations. In particular, a break-up of the mass distribution into a disk + a halo around the disk is probably needed for both luminous and dark matter components.

In addition to analytic approaches, numerical calculations/simulations in 2D polar coordinates are fruitful in relating mass models to observations.

It is not clear if general relativistic treatment, normally needed for high gravitational fields, gives anything more than Newtonian dynamics, but is worth exploring further.

Notes added in proof: (1) For an exposition on how a rotation curve is derived from the observations of a disk galaxy velocity field on the sky, deprojecting for disk inclination, see Teuben⁵⁷. (2) Over the years there have been attempts to derive radial disk mass distributions from observed rotation curves. Two numerical schemes are described in the article. Another semi-analytic attempt is by Feng and Gallo⁵⁸, who also refer to a series of numerical calculations by K. F. Nicholson. All these independent studies do not need dark matter. (3) For an update on MoND after Sanders and McGaugh⁴⁴, see Bekenstein⁵⁹. (4) Finally, a fundamental theory purporting to show that dark matter, dark energy and the accelerating universe are artefacts of our 3 + 1 dimensional perspective on a pre-geometric structure based on ‘process physics’ has been developed by Cahill⁶⁰.

1. Grupen, C., *Astroparticle Physics*, Springer, 2005.
2. Banhatti, D. G., Large-scale structure in the universe. *Curr. Sci.*, 1993, **65**, 827–835; *Cosmography, Phys. Educ.*, 1994, **11**, 175–183; Early universe and present large-scale structure – Part 1. *Phys. Educ.*, 1998, **15**, 273–282; Early universe and present large-scale structure – Part 2. *Phys. Educ.*, 2000, **17**, 161–170.
3. Spergel, D. N. *et al.*, First year WMAP observations. *Astrophys. J. Suppl.*, 2003, **148**, 175–194; WMAP three-year observations, 2007, astro-ph/0603449v2.
4. Faucher-Giguere, C.-A. *et al.*, Numerical simulations unravel the cosmic web. *Science*, 2008, **319**, 52–55; Navarro, J. F. *et al.*, A universal density profile from hierarchical clustering. *Astrophys. J.*, 1997, **490**, 493–508; Kamionkowski, M. and Kouhiappas, S. M., Galactic substructure and direct detection of dark matter, 2008, arXiv:0801.3269 astro-ph.
5. Fields, B. D. and Sarkar, S., Big bang nucleosynthesis, 2003, astro-ph/0406663v1 (In Eidelman, S. *et al.*, *Phys. Lett. B*, 2006, **592**, 1–1109 [<http://pdg.lbl.gov>] (Particle Data Group)).
6. Gaitskell, R. J., Direct detection of dark matter. *Annu. Rev. Nucl. Part. Sci.*, 2004, **54**, 315–359; Krauss, L. M., Dark matter candidates – What’s cold... and what’s not, 2007, astro-ph/0702051v1; Bottino, A. and Fornengo, N., Dark matter and its particle candidates, 1999, astro-ph/9904469; Bertone, G. *et al.*, Particle dark matter – Evidence, candidates and constraints. *Phys. Rep.*, 2005, **405**, 279–390; Ellis, J., Particle candidates for dark matter. *Phys. Scr.*, 2000, **T85**, 221–230; Kamionkowski, M. and Kouhiappas, S. M., Galactic substructure and direct detection of dark matter, 2008, arXiv:0801.3269 astro-ph.
7. Méra, D., Mizony, M. and Baillon, J.-B., Disk surface density profile of spiral galaxies and maximal disks, Preprint (submitted to *Astron. Astrophys.*, and *Mon. Not. R. Astron. Soc.*), 1996/97.
8. de Boer, W. *et al.*, EGRET excess of diffuse galactic gamma rays as tracer of dark matter. *Astron. Astrophys.*, 2005, **444**, 51–67: [See also de Boer, W., Do gamma rays reveal our galaxy’s dark matter? *CERN Courier*, December 2005, **45**, 17–19].
9. Xu, Y. *et al.*, The distance to the Perseus spiral arm in the Milky Way. *Science*, 2006, **311**, 54–57; supporting online material.
10. Hachisuka, K. *et al.*, Water maser motions in W3(OH) and a determination of its distance. *Astrophys. J.*, 2006, **645**, 337–344 (also astro-ph/0512226).
11. Mel’nik, A. M., Outer pseudo ring in the Galaxy. *Astron. Lett.*, 2006, **32**, 7–13 [translated from the Russian, *Pis’ma Astron. Zh.* 2006, **32**, 9–15].
12. Rix, H.-W. and Zaritsky, D., Nonaxisymmetric structures in the stellar disks of galaxies. *Astrophys. J.*, 1995, **447**, 82–102.
13. Dekel, A., Lost and found dark matter in elliptical galaxies. *Nature*, 2005, **437**, 707–710.
14. Aharonian, F. *et al.*, Discovery of very-high-energy γ -rays from the Galactic Centre ridge. *Nature*, 2006, **439**, 695–698; *Phys. Rev. Lett.*, 2006, **97**, 221102.
15. Ando, S., Cosmic γ -ray background from dark matter annihilation. *J. Phys.*, 2007, **60**, 247–250.
16. Shu, F. H., *The Physical Universe: An Introduction to Astronomy*, University Science Books, 1982 or 1985.
17. Binney, J. and Tremaine, S., *Galactic Dynamics*, Princeton University Press, 1987.
18. Fish, V. L. *et al.*, H I absorption toward ultracompact H II regions – Distances and galactic structure. *Astrophys. J.*, 2003, **587**, 701–713.
19. Sofue, Y. and Rubin, V., Rotation curves of spiral galaxies. *Annu. Rev. Astron. Astrophys.*, 2001, **39**, 137–174.
20. Carollo, D. *et al.*, Two stellar components in the halo of the Milky Way. *Nature*, 2007, **451**, 1020–1025 (erratum in the 10 January 2008 issue).
21. Caldwell, J. A. R. and Ostriker, J. P., The mass-distribution within our galaxy – A 3 component model. *Astrophys. J.*, 1981, **251**, 61–87.
22. Cowsik, R. *et al.*, Dispersion velocity of Galactic dark matter particles. *Phys. Rev. Lett.*, 1996, **76**, 3886–3889.
23. Dehnen, W. and Binney, J., Mass models of the Milky Way. *Mon. Not. R. Astron. Soc.*, 1998, **294**, 429–438.
24. Ryder, S. D. *et al.*, An H I study of the NGC6744 system. *Publ. Astron. Soc. Aust.*, 1999, **16**, 84–88.
25. Sanders, R. H., The published extended rotation curves of spiral galaxies: Confrontation with modified dynamics. *Astrophys. J.*, 1996, **473**, 117–129.
26. Courteau, S., Optical rotation curves and linewidths for Tully–Fisher applications. *Astron. J.*, 1997, **114**, 2402–2427.
27. Martín, M. C., Catalogue of H I maps of galaxies. II. Analysis of the data. *Astron. Astrophys. Suppl.*, 1998, **131**, 77–87; Catalogue of H I maps of galaxies. *Astron. Astron. Suppl.*, 1998, **131**, 73–75 (only available in electronic form at the CDS via anonymous ftp: 130.79.128.5 or <http://cdsweb.u-strasbg.fr/Abstract.html>).
28. Catiniella, B. *et al.*, Template rotation curves for disk galaxies. *Astrophys. J.*, 2006, **640**, 751–761 (also astro-ph/0512051).
29. Persic, M. *et al.*, The universal rotation curve of spiral galaxies – I. The dark matter connection. *Mon. Not. R. Astron. Soc.*, 1996, **281**, 27–47.
30. Bosma, A., Dark matter in disc galaxies, 1998, astro-ph/9812013v1.
31. Narayan, C. A. and Jog, C. J., The puzzle about the radial cut-off in galactic discs. *Astron. Astrophys.*, 2003, **407**, L59–L62.
32. Kundt, W., In 11th Marcel Grossmann Meeting WSPC Proceedings: The proposed black holes around us, 2007.
33. Saslaw, W. C., *Gravitational Physics of Stellar and Galactic Systems* (especially section 59), Cambridge University Press, 1985.
34. Graneau, P. and Graneau, N., *Newton versus Einstein: How Matter Interacts with Matter*, Carlton/Affiliated East-West, New Delhi, 1993.
35. Banhatti, R. D. and Banhatti, D. G., *Phys. Edu. (India)*, 1996, **12**, 377–379: Book review of (34) Graneau & Graneau, 1993.
36. Mestel, L., On the galactic law of rotation. *Mon. Not. R. Astron. Soc.*, 1963, **126**, 553–575.
37. Byrd, G. *et al.*, Dynamical friction on a satellite of a disc galaxy. *Mon. Not. R. Astron. Soc.*, 1986, **220**, 619–631.

-
38. Miller, R. H., On the stability of disk-like galaxies in massive halos. *Astrophys. J.*, 1978, **224**, 32–38; Numerical experiments on the stability of disk-like galaxies. *Astrophys. J.*, 1978, **223**, 811–823; Validity of disk galaxy simulations. *J. Computat. Phys.*, 1976, **21**, 400–437; Stability of a disk galaxy. *Astrophys. J.*, 1974, **190**, 539–542; Partial iterative refinements. *J. Comput. Phys.*, 1971, **8**, 464.
39. Valtonen, M. J. *et al.*, Dynamical friction on a satellite of a disk galaxy: The circular orbit. *Celestial Mech. Dyn. Astron.*, 1990, **48**, 95–113.
40. Vallée, J. P., Galactic magnetism and the rotation curves of M31 and the Milky Way. *Astrophys. J.*, 1994, **437**, 179–183.
41. Robin, A. C. *et al.*, The radial structure of the galactic disc. *Astron. Astrophys.*, 1992, **265**, 32–39.
42. Méra, D. *et al.*, Towards a consistent model of the Galaxy. II. Derivation of the model. *Astron. Astrophys.*, 1998, **330**, 953–962.
43. Gentile, G. *et al.*, The cored distribution of dark matter in spiral galaxies. *Mon. Not. R. Astron. Soc.*, 2004, **351**, 913–922.
44. Sanders, R. H. and McGaugh, S. S., Modified Newtonian dynamics as an alternative to dark matter. *Annu. Rev. Astron. Astrophys.*, 2002, **40**, 263–317.
45. Zhao, H. S., Coincidences of dark energy with dark matter – Clues for a simple alternative? 2007, arXiv:0710.3616v2 astro-ph.
46. Cooperstock, F. I. and Tieu, S., General relativity resolves galactic rotation without exotic dark matter, 2005, astro-ph/0507619. See also Perspectives on galactic dynamics via general relativity, 2005, astro-ph/0512048; Galactic dynamics via general relativity – A compilation and new developments, 2006, astro-ph/0610370.
47. Vogt, D. and Letelier, P. S., Presence of exotic matter in the Cooperstock and Tieu galaxy model, 2005, astro-ph/0510750. Also Exact general relativistic rotating disks immersed in rotating dust generated from van Stockum solution, 2006, astro-ph/0611428.
48. Korzyński, M., Singular disk of matter in the Cooperstock–Tieu galaxy model, 2005, astro-ph/0508377.
49. Cross, D. J., Comments on the Cooperstock–Tieu galaxy model, 2006, astro-ph/0601191.
50. Fuchs, B. and Phelps, S., Comment on (46) Cooperstock and Tieu (2005a). *New Astron.*, 2006, **11**, 608–610.
51. Vogt, D. and Letelier, P. S., Relativistic models of galaxies. *Mon. Not. R. Astron. Soc.*, 2005, **363**, 268–284.
52. Balasin, H. and Grumiller, D., Significant reduction of galactic dark matter by general relativity, 2006, astro-ph/0602519.
53. Letelier, P. S., Rotation curves, dark matter and general relativity. In *IAU Symposium 238*, 2006, p. 401.
54. González, G. A. and Letelier, P. S., Rotating relativistic thin disks. *Phys. Rev. D*, 2000, **62**, 064025.
55. Yourgrau, P., *A World without Time: The Forgotten Legacy of Gödel and Einstein*, Basic Books, 2005.
56. Banhatti, D. G., Review of the book, ‘A word without time: The forgotten legacy of Gödel and Einstein’ by Palle Yourgrau. *Curr. Sci.*, 2006, **90**, 1694.
57. Teuben, P. J., Velocity fields of disk galaxies. In *Disks of Galaxies: Kinematics, Dynamics & Perturbations* (eds Athanassoula, E. and Bosma, A.), ASP Conference Series, 27 April 2002, arXiv: astro-ph/020447v1.
58. Feng, J. Q. and Gallo, C. F., Galactic rotation described with thin-disk gravitational model, 4 March 2008, arXiv:0803.0556v1 [astro-ph].
59. Bekenstein, J. D., The modified Newtonian dynamics – MOND and its implications for new physics, 27 March 2007, arXiv:astro-ph/0701848v2.
60. Cahill, R. T., A quantum cosmology: No dark matter, dark energy nor accelerating universe, 18 September 2007, arXiv:0709.2909v1 [physics.gen-ph].

ACKNOWLEDGEMENTS. I thank Prof. Dr Wim de Boer for inviting me to Karlsruhe, Germany for a visit and a seminar. University of Münster, Germany provided general facilities and use of library. Part of the work was done while visiting Institute of Mathematical Sciences (MatScience), Chennai, where I also gave a seminar on the topic. Department of Theoretical Physics, University of Madras also arranged my seminar on this topic. Nora Loiseau’s comments at various stages improved clarity. Prof. Wolfgang Kundt, Bonn, Germany provided valuable comments. Prof. Peter Boschan, Münster encouraged me by discussing relevant matters and lending books when needed. I also thank the referees for their valuable suggestions. Finally, I thank Dr Radha D. Banhatti for encouragement and critical comments on various versions of the article.

Received 9 March 2007; revised accepted 24 February 2008
